Reprinted from

JAPANESE JOURNAL OF
APPLIED
PHYSICS

REGULAR PAPER

A Micrograting Sensor for DNA Hybridization and Antibody Human Serum Albumin–Antigen Human Serum Albumin Interaction Experiments

Naphat Chathirat, Nithi Atthi, Charndet Hruanun, Amporn Poyai,
Suthisa Leasen, Tanakorn Osotchan, and Jose H. Hodak

Jpn. J. Appl. Phys. **50** (2011) 01BK01

Japanese Journal of Applied Physics **50** (2011) 01BK01 **REGULAR PAPER**
DOI: 10.1143/JJAP.50.01BK01

A Micrograting Sensor for DNA Hybridization and Antibody Human Serum Albumin–Antigen Human Serum Albumin Interaction Experiments

Naphat Chathirat*, Nithi Atthi[1], Charndet Hruanun[1], Amporn Poyai[1], Suthisa Leasen[2], Tanakorn Osotchan, and Jose H. Hodak[3]

Materials Science and Engineering Program, and Capability Building Unit in Nanoscience and Nanotechnology, Faculty of Science, Mahidol University, Bangkok 10400, Thailand
[1]*Thai Microelectronics Center, National Electronics and Computer Technology Center, Chacheongsao 24000, Thailand*
[2]*Physics Department, Faculty of Science, Mahidol University, Bangkok 10400, Thailand*
[3]*INQUIMAE-DQIAyQF, Facultad de Ciencias Exactas y Naturales, Universidad de Buenos Aires, Buenos Aires 1428, Argentina*

Received June 24, 2010; revised October 16, 2010; accepted October 26, 2010; published online January 20, 2011

A biosensor structure comprising silicon nitride (Si_3N_4) micrograting arrays coated with a spin-on-glass (SOG) material was investigated. This grating structure was located on a silicon groove, which was etched by a deep reactive ion etching (DRIE) process. The biosensor was used as a specific detector of DNA molecules and antibody–antigen interactions. In our DNA sensing experiments, the first step was the activation of the grating surface with amine functional groups, followed by attachment of a 23-base oligonucleotide probe layer for hybridization with a complementary target DNA. The sensing device was tested for detecting specific antigen/antibody interactions for human serum albumin (HSA) and antigen bovine serum albumin (BSA). The readout system consisted of a white light lamp that illuminated a small spot on the grating surface at normal incidence through a fiber optic probe with a spectrometer used to collect the reflected light through a second fiber. We show that these sensing devices have the capability to detect DNA as well as antigen–antibody binding for HSA. The detection sensitivity for HSA was better than that for DNA mainly owing to the larger size and concomitant refractive index changes upon binding to the sensor. We show that it is possible to quantify the amount of biomolecules bound to the grating surface by measuring the wavelength shift of the reflectance spectra upon exposure to the samples.

1. Introduction

Optical bioelectronic devices or optical biosensors have been developed into powerful analytical tools in fields of healthcare, pharmaceutical industry, environmental monitoring, homeland security, and warfare.[1)] The optical biosensors use a light source for the transduction of a biochemical interaction into a measurable change in light transmission or reflection. One of the most popular optical biosensor techniques is surface plasmon resonance (SPR) spectroscopy which measures refractive index changes at an interface between metal and dielectric materials by evanescent field excitation.[2–5)] Other methods commonly used with optical biosensors are based on reflectometric interference spectroscopy (RifS)[6,7)] which measures the refractive index of a substance or biological layer via interferometry.[8,9)] The theoretical detection limits of these methods have been experimentally confirmed to be feasible for concentration ranges that are relevant for the diagnosis of diseases. While SPR and RifS are sensitive, they usually require flow systems and moderate sample sizes and allow a single analyte to be quantified in a given experiment. Therefore, they are not easy to integrate into the microarray type of quantification setups for simultaneous sampling and analyte sensing with a high throughput.

In this paper, we describe an approach for detecting molecular interactions by utilizing a diffraction grating surface and a series of selected dielectric materials or membranes acting as a surface binding platform. Upon illumination with polychromatic light, the reflectance spectra show characteristic interference fringes at wavelengths that shift when biomolecules bind to the membrane. The introduction of specific biomolecules on top of the platform membrane alters the optical path of the reflected light in such a way that the maxima and minima suffer a distinct wavelength shift.[10,11)] The complementary binding molecules can thus be detected without using any fluorescent or particle labels. This technique does not depend on the changing of the bio-molecular binding, and can be performed by dropping a sample directly on the grating surface. This approach senses the change of the optical path down to nanometers therefore, the sensitivity of the sensor is sufficient to differentiate between an original sensing layer without hybridization and complimentary hydridized layers.

2. Materials and Methods

2.1 Micrograting structure fabrication

Biosensor fabrication was carried out by using a 6-in. p-type ⟨100⟩ silicon (Si) wafer as a substrate. Figure 1 shows the sequence of microfabrication steps on the right side (from top to bottom). A 500 nm thick silicon dioxide (SiO_2) film was deposited onto the silicon surface by a thermal oxidation method. Next, an additional SiO_2 film was deposited with plasma-enhanced chemical vapor deposition (PECVD) technique on both sides of the Si substrate reaching 1.5 μm on the front side and 4.5 μm on the back surface. We term this PECVD-SiO_2 film as PEOX film here after. The 4.5 μm PEOX film on the back surface of the Si wafer acted as a hard mask during the deep etching process. After depositing the PEOX film on the substrate, it was densified in a thermal furnace. A 180 nm thick layer of silicon nitride (Si_3N_4) was deposited on the front surface of the Si substrate using the PECVD technique. The refractive index of the Si_3N_4 film was initially 2.010. Photolithography and reactive ion etching (RIE) processes were used to fabricate a square lattice micrograting pattern on the Si_3N_4 and PEOX film stack. The pillar size and the space between the pillars was 1 μm. This grating structure generated a 2 μm line spacing and 50% filling. Then, another SiO_2 film was deposited on the Si_3N_4 grating structure using a spin-on-glass (SOG) technique. The SOG film had a thickness of 280 nm and acted as a dielectric material that filled-in the space between

*E-mail address: g5137662@student.mahidol.ac.th

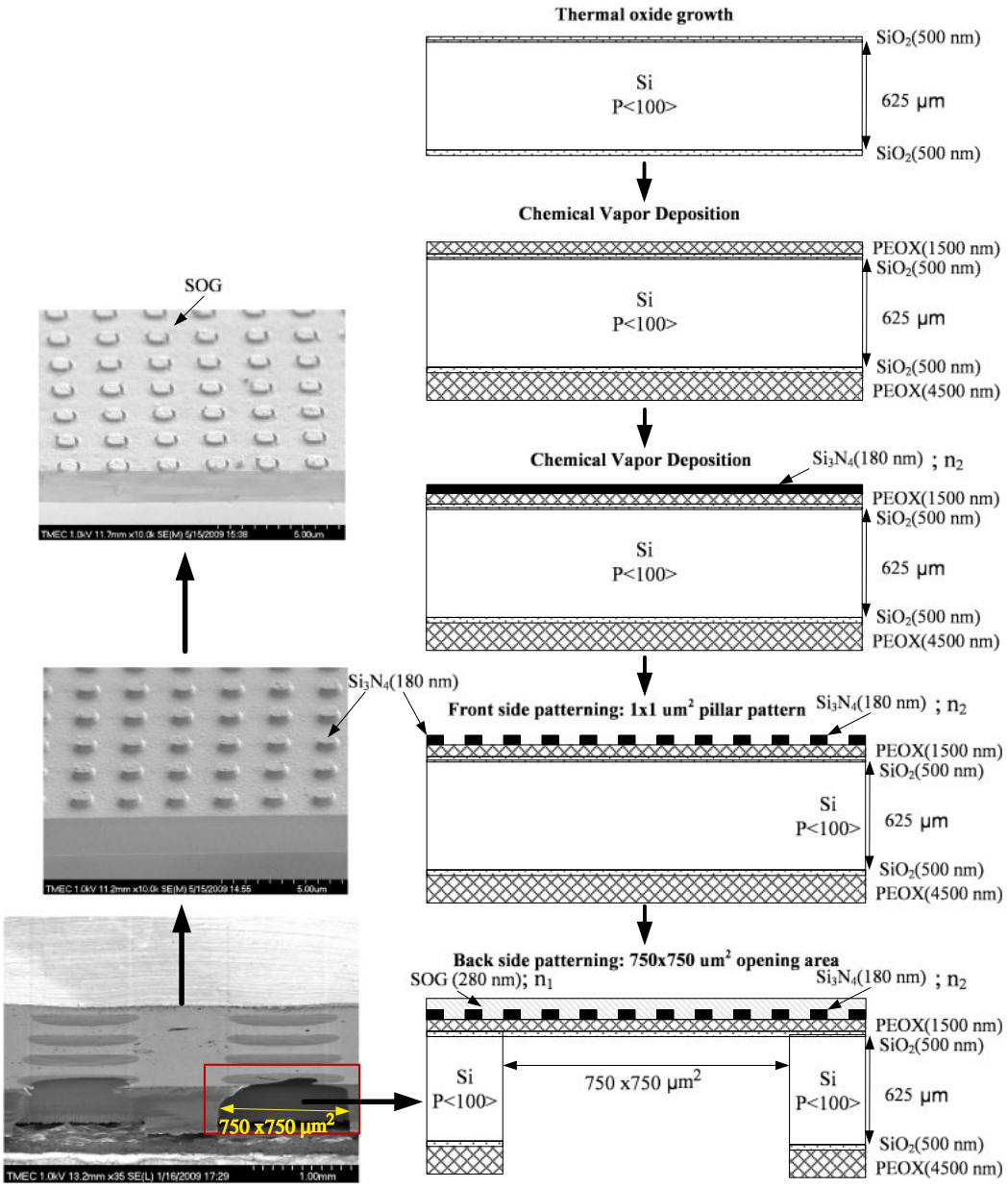

Fig. 1. (Color online) Cross-sectional SEM image after DRIE through Si wafer and micrograting construction processes.

the Si_3N_4 pillars. After that, the SOG film was cured at 400 °C for 30 min. The quality of the SOG film, as characterized by the index of refraction, was measured using an ellipsometer. As a result of embedding the micrograting in the SOG SiO_2 layer, the effective refractive index of the Si_3N_4/SiO_2 stratum was 1.413, considering the average of the whole array. Scanning electron microscope (SEM) photographs of the micrograting structure with Si_3N_4 pillars patterned on a dielectric material after etching the back side of the Si wafer while masking the front surface of the wafer are shown in Fig. 1, bottom left panels.

On the backside structure, a photolithography process was used to pattern a $750 \times 750\,\mu m^2$ open window on the PEOX film. Then, a 4500 nm thick PEOX film of Si was etched on the back surface by using an RIE process. Next, the Si substrate was etched using a deep reactive ion etching (DRIE) technique. The total etch depth into the Si substrate was equal to the thickness of the Si wafer, that is 625 μm thick. During the DRIE step, the remaining photoresist material and the 4500 nm thick PEOX act as a hard mask to prevent the Si layer from being etched away. The DRIE process etched away the Si material until it reached the SiO_2 TOX film on the front side of the Si. The final structure is shown in Fig. 1.

2.2 Bio-molecular layer

2.2.1 DNA immobilization and hybridization

After the micrograting structure was fabricated, the receptor molecules were immobilized on its surface following the steps shown in Fig. 2. First, the grating surface was cleaned by immersion in a sodium hydroxide (NaOH) solution of 7% for 30 s and soaked in deionized water for 1 min. Second, the grating was soaked in water for 30 min to create –OH (hydroxyl group) and washed with ethanol for 15 min after which it was immersed for 10 min in a solution of 3-aminopropyltriethoxysilane (APTES) mixed with acetone at a ratio of 3 : 47 (by volume).[12–14] Finally, the grating surface was dried in a convection oven at 50 °C for

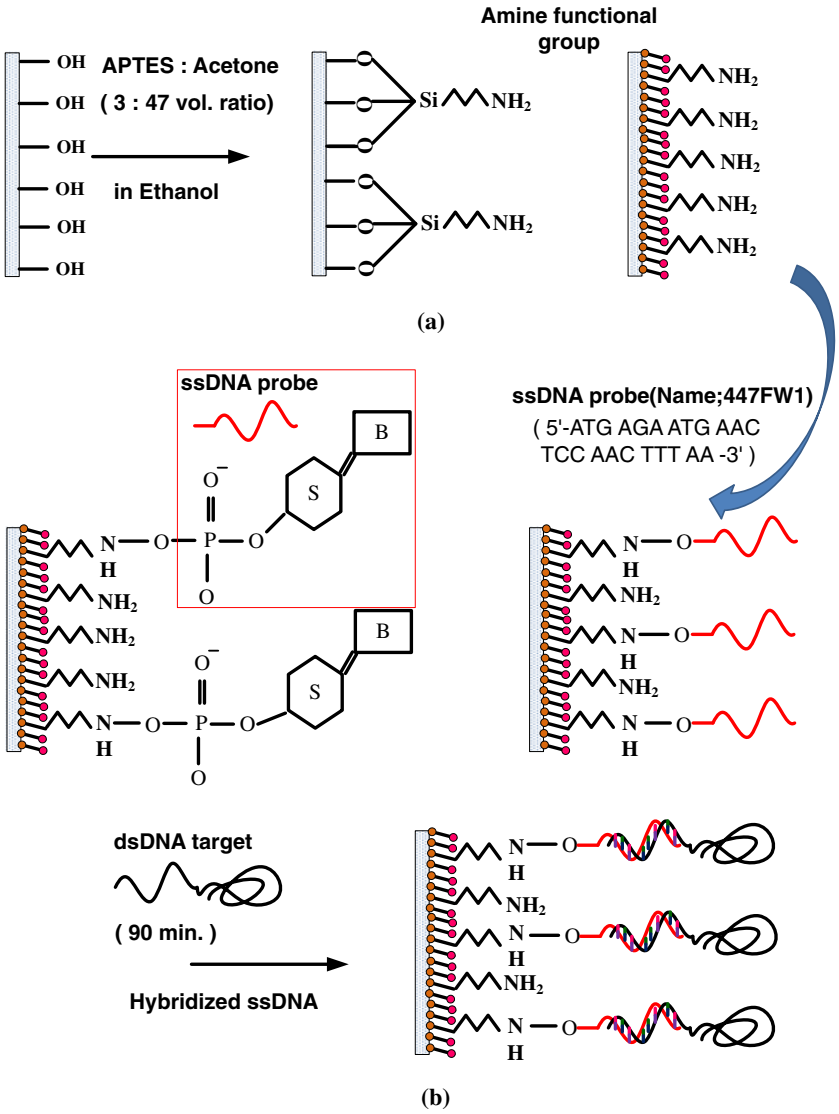

Fig. 2. (Color online) Surface modification of the grating sensor for DNA (a) APTES on the grating surface and (b) DNA immobilization and hybridization on APTES surface.

60 min.[15] In this method, the amine functional groups (NH_2-terminal) were deposited onto the grating surface, as shown in Fig. 2(a). The NH_2-terminated surface ($pK_a \sim 10$) is in the protonated form at a pH of 7.4 which allows the binding of DNA molecules via electrostatic interaction with their negative phosphate backbone.[15–20] Before the deposition of ssDNA, the grating was immersed for 10 min in a solution containing 0.3 M sodium chloride and 0.015 M sodium acetate having a pH of 7.0 (2xSSC). The ssDNA oligonucleotide probes used were 23 bases in length. The sequence of this ssDNA was 5′-ATG AGA ATG AAC TCC AAC TTT AA-3′. The grating was coated with 5 µl of a ssDNA solution having a concentration of 10^{13} copies/µl and dried in air for 1 h. Finally, the surface was cleaned by immersion for 10 min in the 2xSSC solution, soaked in deionized water for 5 min, and dried under atmospheric conditions. After that, the optical properties of the obtained DNA probe surface were measured immediately.

For hybridization of the DNA molecules, one biosensor structure with the ssDNA probe attached had 1,447 oligonucleotide double stranded DNA targets with a concentration of 10^1 copies/µl for a total of 5 µl was dropped onto the DNA probe surface and dried for 90 min. An identical second biosensor had the double stranded DNA targets but at a concentration of 10^3 copies/µl for a total of 5 µl dropped on it. Then, both DNA targets were cleaned with 2xSSC solution for 10 min and soaked in deionized water for 5 min and then dried under atmospheric conditions. The optical properties of the devices that have the DNA targets bound to them were measured immediately after drying. A comparison between the two DNA targets with their signal outputs is shown in the results. The structure after hybridization is shown in Fig. 2(b).

2.2.2 Antibody–antigen HSA protein

In the assays for protein detection, human serum albumin (HSA) was chosen because it is the most abundant protein in human blood plasma. The antibody HSA terminal can be attached to the NH_2-terminal or amine functional group in a sequence of steps similar to that described for DNA immobilization. Therefore, the antibody–antigen HSA binding could also be tested on the same type of sensor device. The process of immobilization of HSA is summarized in Fig. 3. First, the activation of the grating surface with

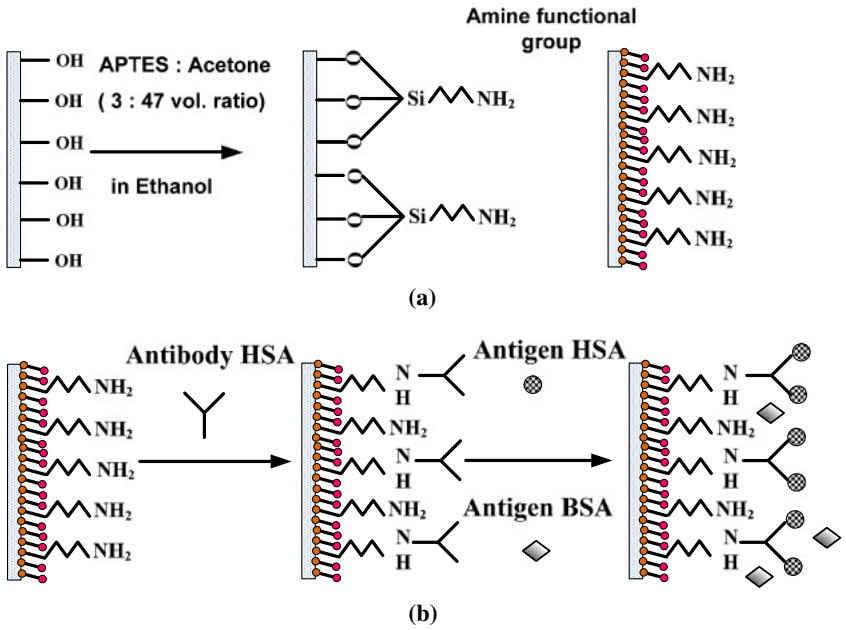

Fig. 3. (Color online) Surface modification of the grating sensor for proteins (a) APTES on the grating surface and (b) antibody–antigen HSA of protein attached onto APTES.

APTES molecules was performed as described previously to obtain the NH_2-terminated surface. Second, the modified grating surface was immersed in a phosphate buffered solution (PBS) for 10 min. PBS used was a mixture of NaCl, KCl, Na_2HPO_4, KH_2PO_4, and DI water at a ratio of 40 g : 1 g : 14.5 g : 1 g : 800 ml, respectively. Third, a 5 µl aliquote of the antibody HSA solution with a concentration of 5 mg/ml, was dropped onto the surface and left to dry for 2 h at room temperature. The grating was then rinsed with PBS (pH = 7.4) for 10 min, soaked in DI water for 5 min, and dried at room temperature. Finally, the optical properties of the obtained antibody HSA surface were measured immediately after the last drying step. In this study, an antigen–antibody bovine serum albumin (BSA) solution was used for nonspecific recognition in the experiments.

A 10 µl aliquote of the antigen HSA with a concentration of 1 mg/ml was dropped on the grating surface and left to dry for 2 h followed by a washing step by immersion in a PBS solution for 10 min, soaked in DI water for 5 min, and then dried under atmospheric conditions [Fig. 3(b)].

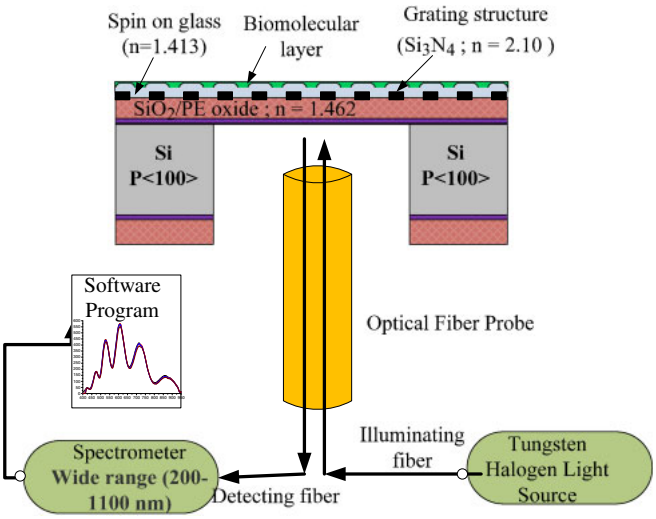

Fig. 4. (Color online) Schematic diagram of the instrumentation used to illuminate and read the signal from biosensor.

2.2.3 Sensor readout instrumentation

A schematic diagram of the system used to illuminate the sensor and to detect the reflected signal is shown in Fig. 4. The setup consisted of (1) an LS-1 versatile tungsten halogen light source with emission in the range of 360 to 2,500 nm, and (2) a CCD spectrometer (Ocean Optics HR2000CG-UV-NIR) with detection in the range of 200 to 1,100 nm at an optical resolution of 1.0 nm. The light was coupled into and out of the gratings via a fiber optic reflection/backscattering probe in order to measure diffused light reflectance from the surface. The fiber probe consisted of a tight bundle of seven optical fibers in a stainless steel ferrule with six illuminating fibers and one collection fiber. With this apparatus, the spectrometer integrates the reflected light signal every 20 ms in each measurement. The illumination comes from the back side of the grating structure through a $750 \times 750\,\mu m^2$ opening window. During the experiment, a small spot of the grating is illuminated at normal incidence through a fiber optic probe, and then the spectrometer collects the reflected light through the second fiber, which is also at normal incidence. Therefore, a single spectrometer reading is performed within a time scale of a few milliseconds making it possible to quickly measure a large number of molecular interactions taking place in parallel on the grating surface. The binding of materials with indices of refraction that differ from the effective refractive index of the grating generates distinct shifts in the position of the reflectance spectrum. In this work, using the low refractive index SOG material effectively enables the detection of the low refraction index biomaterial layers.

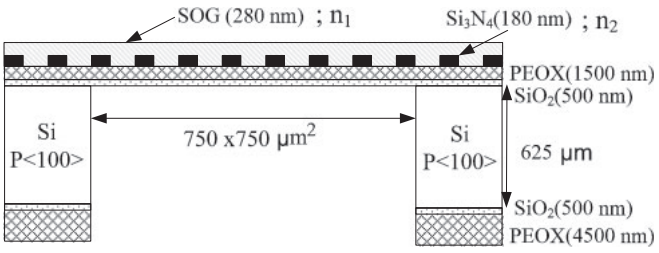

Fig. 5. Schematic diagram of micrograting structure.

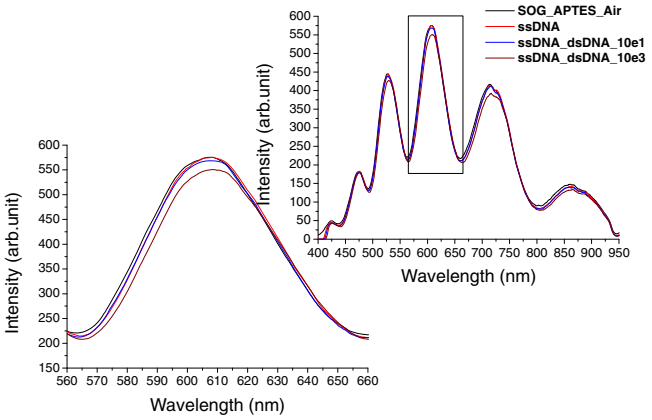

Fig. 6. (Color online) Reflectance spectra for the grating sensor after APTES, ssDNA, and dsDNA surface modification.

3. Results and Discussion

3.1 Biosensor structure and principle of operation

Figure 5 shows a schematic of the sensing devices. Light can be seen on the front side of the structure when the back side is illuminated because of the extremely thin grating structure here used. The Si_3N_4 grating structure, after being coated with the SOG film (top left panel in Fig. 1). The coating appears to be homogeneous over the length scale of the grating. Upon normal incidence, the light delivered by the optical fibers propagates through the device. A portion of the light reflected back at the top interface returns, and it is detected by the collection fiber. In doing so, the light propagates across the film of biomolecules that are bound on top. As the light propagates backwards, it interferes with the light reflected at the grating, causing a series of interference fringes to appear in the spectrum of the light collected by the fiber.[21] Since the light has to propagate across the biomolecule layer, the phase shift accumulated in the light that is reflected at the topmost interface depends on the refractive index and the thickness of that layer.[22,23] Thus, the maxima of interference will appear when the condition

$$2nd = m\lambda, \quad (1)$$

where m is an integer for interference maxima and a half integer for the interference minima, and n and d are the refractive index and the thickness of the biomolecular layer, respectively. Changes in the thickness or refractive index of the layer of biomolecules can thus be readily detected by monitoring the shift in the position of the maxima and minima of interference.[22]

3.2 Hybridization of DNA molecules

This optical biosensor device was used to detect DNA hybridization. The spectral measurements were carried out on individual gratings; thus, the intensity of the light detected varied slightly from device to device owing to the variation in fiber positioning. Owing to these fluctuations, the detected intensity was not utilized as a quantitative measurement of the sensor response. The operation as a DNA hybridization biosensor relies on the complementary coupling between the specific ssDNA sequences in the substrate and in the target DNA. The response of the biosensor depends on the amount of the DNA that attaches to the grating surface via the mechanism represented in Figs. 2 and 3. The reflection spectra of the surfaces at the various modification stages are shown in Fig. 6. The top right panel in Fig. 6 shows the whole spectrum, and the lower right panel shows a selected fringe where the largest shifts occurred. Starting from the APTES modification, there is almost no shift in the reflection spectrum relative to that in bare SOG coated grating. Upon binding the ssDNA layer, a small shift occurs. At the concentrations used here, *ca.* 10^{13} copies/μl, there is enough ssDNA to form more than one monolayer. However, once all the amine groups on the surface are bound to the phosphate groups of the DNA, the surface acquires a net negative charge, which effectively suppresses further ssDNA binding. Therefore, a single monolayer of ssDNA binds. Assuming that the ssDNA binds using as many phosphate groups as possible, the thickness of this layer should be about one ssDNA helix diameter *ca.* 4.5 nm. The small shift observed upon the formation of this layer is consistent with a small difference in the refractive index between the APTES modified grating ($n = 1.46$)[24] and that for the ssDNA layer, which is approximately 1.50.[25]

When complementary target ssDNAs are added, they bind to the probe ssDNA on the surface, and the shift observed depends on the amount of DNA that hybridized to the device. Because dsDNA is a large molecule due to the target chain length (1447 bases) a large shift is observed. Although the hybridized target of 10^1 copies/μl was not enough for full grating coverage, the spectrum significantly differs from that for ssDNA, confirming the hybridization event. Figure 7 shows the device response to varying concentrations of target DNA. Although the correlation is not linear, the spectral shifts accompany the amount of target ssDNAs present in the solution. We find an approximately linear relationship between the logarithm of the number of copies in the sample and the spectral shift for concentrations larger than *ca.* 10 copies/μl. This makes these devices useful for the detection of DNA in polymerase chain reaction amplification schemes.

3.3 Antigen–antibody interaction

To investigate the micrograting response to the antigen–antibody interaction, we exposed the grating carrying immobilized antibodies for HSA to a solution of the antigen. The interference fringes of our biosensor shown in the upper right panel of Fig. 8, significantly shift in each surface modification step, reflecting changes of refractive indices and thickness of the biomolecular layer. The fringe wavelength changed when the biomolecular materials were deposited or removed from the grating surface. The

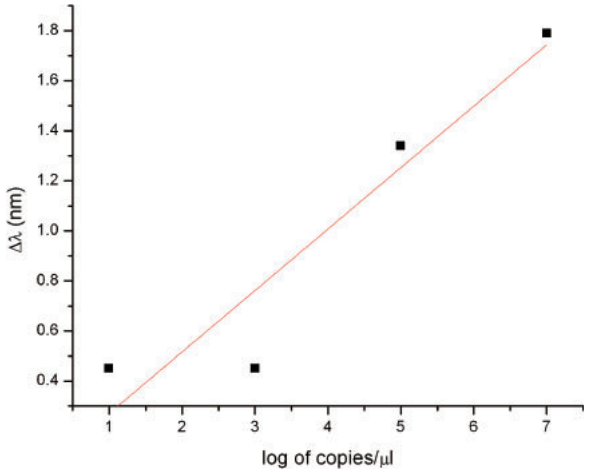

Fig. 7. (Color online) Variation of the spectral shift with the concentration of target DNA in the DNA-sensing grating device.

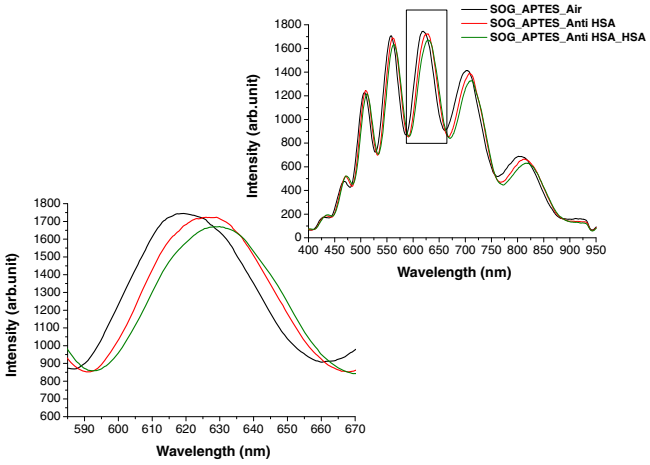

Fig. 8. (Color online) Reflectance spectra for the grating sensor after APTES and protein surface modifications.

wavelength red-shifted when the thickness of HSA was increased. When HSA was removed, the wavelength blue-shifted back to the original value. This means that the shift can be accounted for by the adhesion of the target substance. As we did in the DNA sensing experiments, we focus on a single fringe for studying changes in the spectra due to specific binding of antibody–antigen. We have chosen to monitor the shifts in the maximum shown in the lower left corner of Fig. 8. The amount of the HSA antibody, which has a molecular weight of 67 kDa is just enough to form one full monolayer on the grating, causing a 4.0 nm shift. The antigen (HSA) has a molecular weight of 150 kDa. Therefore, at 5 mg/ml, there is not enough protein to form a full monolayer on our devices. Because of the larger difference in the refractive index of the protein ($n \sim 1.57$), a 6.7 nm spectral shift is observed relative to the bare APTES-modified grating. In general, the antigen–antibody interaction experiments we carried out always yielded larger spectral shifts than similar experiments using DNA hybridization, suggesting that this sensing device is more sensitive for detecting protein binding. Therefore, the devices can successfully detect the antigen–antibody binding events.

4. Conclusions

A novel biosensor consisting of a micrograting structure and a Si_3N_4 pillar array on silicon embedded in a thin film of SOG was fabricated and tested. By surface modifications with single-stranded DNA or with antibodies, this device allows the optical detection of the hybridization to a complementary ssDNA and the detection of the antigen–antibody interactions. The binding of biomolecules was transduced into a shift in reflectivity spectra, whose fringes shift upon binding in a fashion that depended on the substance thickness and refractive index of the grating material. This biosensor can be used to detect the presence of a specific biosubstance. Owing to the larger molecular weight and affinity for binding of HSA to its antibody, its detection is more sensitive than that for DNA. The wavelength shift of the reflectivity spectra can be correlated to the amount of biomolecules bound to the grating surface.

Acknowledgments

The authors would like to thank the Commission of Higher Education and Ministry of Education of Thailand for their support. The authors also thanks to Thai Microelectronics Center (TMEC), National Electronics and Computer Technology Center, is acknowledged for the biosensor fabrication. This work was partially supported by Nanotec, NSTDA.

1) R. Narayanaswamy and O. S. Wolfbeis: *Optical Sensors* (Springer, New York, 2004).
2) H. Raether: in *Physics of Thin Films*, ed. G. Hass, M. Fancornbe, and R. Hoilman (Academic Press, New York, 1977) Vol. 9, p. 145.
3) M. J. Jory, P. S. Vukusic, and J. R. Sambles: Sens. Actuators B **17** (1994) 203.
4) C. R. Lawrence, N. J. Geddes, and D. N. Furlong: Biosens. Bioelectron. **11** (1996) 389.
5) L. L. Chan, S. L. Gosangari, K. L. Watkin, and B. T. Cunningham: Apoptosis **12** (2007) 1061.
6) F. Ligler and C. Taitt: *Optical Biosensors: Present and Future* (Elsevier, Amsterdam, 2001).
7) G. Gauglitz, I. W. Gopel, and J. Hesse: *Sensors Update* (Wiley-VCH, Weinheim, 1999).
8) A. Brecht and G. Gauglitz: Biosens. Bioelectron. **10** (1995) 923.
9) W. Huber, R. Barner, C. Fattinger, J. Huebscher, H. Koller, F. Mueller, D. Schlatter, and W. Lukosz: Sens. Acutators B **6** (1992) 122.
10) J. R. Sheats and B. W. E. Smith: *Microlithography Science and Technology* (Taylor & Francis, New York, 1998).
11) G. Chartier: *Introduction to Optics* (Springer, New York, 2005).
12) A. Cunningham: *Analytical Biosensors* (Wiley, New York, 1998).
13) V. S. Lin, K. Motesharei, K. S. Dancil, M. J. Sailor, and M. R. Ghadiri: Science **278** (1997) 840.
14) E. Thrush, O. Levi, W. Ha, K. Wang, S. J. Smith, and J. S. Harris, Jr.: J. Chromatogr. A **1013** (2003) 103.
15) H. Yakota and F. Johnson: Nucleic Acids Res. **25** (1997) 1064.
16) B. Lin, J. Qiu, J. Gerstenmeier, P. Li, H. Pien, J. Pepper, and B. Cunninghan: Biosens. Bioelectron. **17** (2002) 827.
17) L. L. Chan, B. T. Cunningham, P. Y. Li, and D. Puff: IEEE Sens. J. **6** (2006) 1551.
18) C. E. Jordan and R. M. Corn: Anal. Chem. **69** (1997) 1449.
19) F. Morhard, J. Pipper, R. Dahint, and M. Grunze: Sens. Actuators B **70** (2000) 232.
20) G. Jin, P. Tengvall, I. Lundstrom, and H. Arwin: Anal. Biochem. **232** (1995) 69.
21) R. Magnusson and S. S. Wang: Appl. Phys. Lett. **61** (1992) 1022.
22) R. Swanepoel: J. Phys. E **16** (1983) 1214.
23) C. Thirstrup and W. Zong: Sens. Actuators B **100** (2004) 298.
24) P. M. Fauchet: *Device Applications of Silicon Nanocrystals and Nanostructures* (Springer, Tokyo, 2009).
25) G. Rong: Biosens. Bioelectron. **23** (2008) 1572.